International Journal of Innovative
Computing, Information and Control
Volume **17**, Number **6**, December **2021**

 ISSN 1349-4198
pp. **1823–1841**

A MODEL FOR THE RESPONSE OF AN OCCUPANT AND WHEELCHAIR SYSTEM SUBJECTED TO VERTICAL VIBRATIONS

Pongtep Weerapong[1,2], Kotaro Hashikura[3], Md Abdus Samad Kamal[3] and Kou Yamada[3]

[1]Department of Production Technology
Faculty of Industrial Technology
Nakhon Si Thammarat Rajabhat University
M4 Tha-ngow Subdistrict, Maung District, Nakhon Si Thammarat 80280, Thailand
pongtap_wee@nstru.ac.th

[2]Graduate School of Science and Technology
[3]Division of Mechanical Science and Technology
Gunma University
1-5-1 Tenjincho, Kiryu 376-8515, Japan
{ t202b007; k-hashikura; maskamal; yamada }@gunma-u.ac.jp

Received May 2021; revised September 2021

Abstract. *This paper discusses an approach for creating a mathematical model for studying the simulated responses from a 9-DOF occupant and wheelchair system. Outputs were obtained by applying transfer functions of vibration to the mathematically linear model, and the outcomes were examined in order to study the behavior of an operating wheelchair in response to vertical vibrations emanating from the ground on typical traffic surfaces. Transmissibility of vibrations to the wheelchair occupant's anatomy was investigated especially in setups using two different seat cushions with real-world stiffness and damping attributes. The approach employed for this study should be useful in the area of wheelchair suspension design, and for serving as a basis for the future development of more sophisticated, non-linear models.*
Keywords: Mathematical model, Transmissibility, Wheelchair, Vertical vibrations

1. **Introduction.** A body of research and tests conducted on wheelchair users [1] has indicated the need to focus on developing manual wheelchairs with improved performance and increased rider comfort. This area of study has received much attention among designer groups who have investigated the biodynamic responses of wheelchair users in various riding environments ranging from simple on-street rides to journeys on high-speed trains [2]. Of great importance to such efforts, feedback data from the device user will be a key factor towards the successful design of a wheelchair which operates favorably in a range of predictable environments. To that end, various methods have been employed to study the response of wheelchair users; some investigators have even managed to measure users' brainwaves in order to gauge the level of anxiety induced by difficult wheelchair maneuvers [3]. Some interesting studies involving electro-mechanically controlled wheelchairs, such as the work of Budiharto [4] and Mano and Capi [5], have also been published, but those findings are beyond the scope of this paper.

Prolonged exposure to vibrations typical in wheelchair operating environments can lead to anatomical damage on the wheelchair occupant [1, 6-8], especially those vibrations in

DOI: 10.24507/ijicic.17.06.1823

the vertical plane which can result in the most severe health issues [9, 10]. The study of vibrations transmittable to the occupant has therefore become a central concern in the development of the modern wheelchair, especially one that aims to match the user's requirement regarding their comfort and health [11]. From figures derived by us, we focus on the peak vibrations shown therein. Two parameters needing scrutiny here are stiffness and damping. As damper constant increases, the peak vibration is reduced as a result, which signifies a dampening effect on the input excitation.

This paper discusses an approach to generate a mathematical model for studying the mechanical responses of a manual wheelchair suspension system in order to improve upon the current wheelchair design and manufacture, especially in minimizing vibration-induced discomfort to its occupant [6, 12]. The actions and effects of vertical vibrations upon the modelled unit were the prime concern of this investigation. Based on the approaches employed in previous studies [6, 9, 13-15] vibrating forces were to be applied to the model, and their transmission assessed, in order to study the effects between the system parameters and its dynamic response. The ratios of vibration transmissibility were then computed so as to gauge the vibratory sensitivities of the modelled subject in different vibration environments [11, 16, 17], and also in terms of impacts on vital organs of the occupant. The benefit of proper seat cushioning was also studied on two cushion types using real-life values of cushion stiffness and damping parameters [18, 19]. The values of transmissibility thus obtained were then compared with the findings of previous real-life studies [6, 13-15, 20] which had employed wheelchairs with varying seat stiffness and damping properties. This step helped to establish the magnitudes of vibration likely to affect wheelchair occupant's body parts thus leading to physical discomfort and/or health problems. The outcome of this study should help in predicting the behavior of harmful vibrations, thus making the model a useful tool for any future work in the area of wheelchair suspension design.

The model was assigned nine degrees of freedom containing linear lumped parameters of a human form [21-23], seated on a chair-seat suspension padded with two types of cushion. It should be noted that this simulation was confined to evaluating the dynamic response of a human form exposed to vertical vibrations; thus, it is not a general-purpose human biodynamic model. In its simplest form, it is employed to determine the acceleration ratios acting on the model which may then be used for transmissibility testing and comparison of displacement ratios in the study of biodynamic system responses [24, 25]. In most previous studies, investigators tended to pick the threshold frequency range for testing which is the lowest vibration that begins to cause discomfort to the wheelchair occupant. We had already obtained, from their reviews of such literature, a number of working parameters especially those related to stiffness and dashpot. In light of that, we sought to focus more on obtaining additional parameters – such as properties of the tire and seat, from standardized commercially available wheelchairs – for inclusion in the model. The outcomes of our simulations (acceleration or displacement ratios acting on the human figure) were then checked against the results cited in other studies [26, 27] in order to validate the model.

Liang et al. [14] applied 11 degrees of freedom to studying the biodynamic responses of seated pregnant subjects exposed to vertical vibrations in driving conditions. Based largely on Patil's model which divided the occupant's body into three parts, Liang and Chiang [13] compared the biodynamics of a seated posture without backrest support by examining several lumped parameters to determine seat-to-head transmissibility in the same manner as Patil's occupant-tractor system. The system of Patil and Palanichamy [26] had seven degrees of freedom in steady-state vibration with its minimum dynamic response of the body parts in the 0.5 to 11 Hz frequency range. By contrast, Quadros

et al. [28] created a model with 12 degrees of freedom simulating a two-wheeler rider on varying terrain amplitudes, and employed head-to-cab-floor vibrations as input to the model in order to analyze seat responses.

Our literature review confirms that mathematical modelling of the wheelchair-occupant system is well accepted and being increasingly adopted for investigating the biodynamic response of such a system in various vibration environments. Among the studies reviewed, however, there has been none that focuses on the effects of vertical vibrations on the rider of a wheelchair without backrest. We therefore chose to develop a composite model to investigate the transmissibility of vibrations from the ground up, through the body parts of a wheelchair occupant positioned on two types of commercially available seat cushions: Comfort Mate Foam and Meridian Wave. The composite model was formulated as a linear lumped-parameter system with nine degrees of freedom (DOF).

This paper is organized in the following sections. Section 2 analyzes the wheelchair and occupant regarding properties of human tissue, spring and dashpot that constitute the lumped parameters. Section 3 defines force vectors on the masses in free body diagrams. Sections 4 and 5 list out the equations of motion (EOM) in linear form, followed on with their transformation into matrix equations, which are then solved for outputs using transfer functions. Section 6 presents the transmissibility and magnitude ratios as derived from model simulations. Section 7 delivers concluding remarks.

Notations

m	Mass, (kg).	k	Stiffness of the spring, (Ns/m).
c	Damping coefficient, (Ns/m).	$[M]$	Mass matrix.
y	Displacement, (mm).	$[C]$	Damping matrix.
t	Time, (s).	$[K]$	Stiffness matrix.
Q	Impedance, (Ns/m).	k_0	Input stiffness constant.
j	$\sqrt{-1}$, Index.	c_0	Input damping constant.
TR	Transmissibility.	$\{F_0\}$	Input force excitation vector.
ω	Frequency, (rad/s).	H	Transfer function.
$\{y_0\}, \{\dot{y}_0\}$	Displacement and velocity vector of excitation.		
$\{y\}, \{\dot{y}\}, \{\ddot{y}\}$	Displacement, velocity and acceleration vector of response.		

2. **Analysis of Wheelchair-Occupant's Vibrational Response.** Figure 1 is employed for investigating biodynamic responses to vertical vibrations acting on the device in operation. It was modeled with nine DOFs consisting of seven human segments comprising head, back, torso, thorax, diaphragm, abdomen, and pelvis [13, 26], and two masses on the wheelchair representing its seat and chassis & tires. In mechanical terms, these are like springs and dampers and connecting masses of a device. For each mass component subjected to a vertical force, a free body diagram was derived, thus giving rise to a total of nine FBDs. The human figure is in a sitting posture with the lower segment(s) of the body supported by the seat cushion on a traveling wheelchair, while the upper segments unsupported by a backrest. In this configuration, the input vibrations were confined to those coming from the sinusoidal functions of the springs and dampers on the wheelchair tires and emanating through the seat cushion to the occupant's body. The real-world vibrations through the wheelchair foot support were ignored in the model as they were negligibly small in magnitude and affecting only the trunk [29]. Figure 1 shows the model in cross section having nine blocks of mass denoted by m_i, $(i = 1, 2, \ldots, 9)$. The blocks are connected in pairs with a spring and a dashpot whose stiffness and damping coefficients are denoted by k_i and c_i, $(i = 1, 2, \ldots, 9)$.

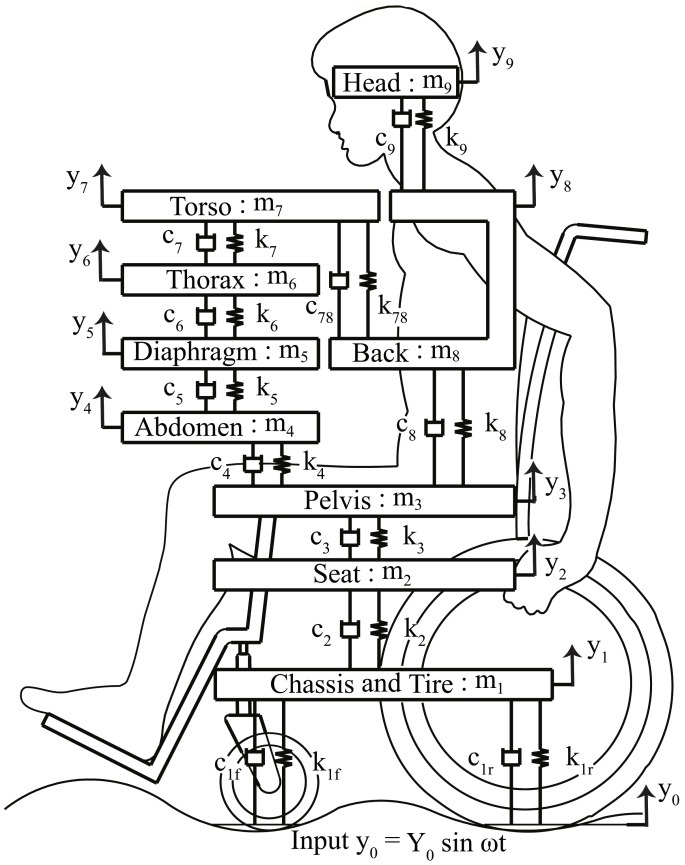

FIGURE 1. Components susceptible to vertical vibrations on the model of seated human body in wheelchair

TABLE 1. Parameter values of manual wheelchair [6, 7]

Mass $[M]$ (kg)	Damping constant $[C]$ (N/m/sec)	Spring constant $[K]$ (N/m)
$m_1 = 16.5$	$c_{1f^*} = 500$	$k_{1f^*} = 60000$
	$c_{1r^*} = 500$	$k_{1r^*} = 6000$
$m_2 = 1.5$	$c_{2a} = 1689$	$k_{2a} = 183200$
	$c_{2b} = 397$	$k_{2b} = 76010$
input amplitude of displacement excitation, $Y_0 = 5$ mm.		

* denotes the parameter value for two tires (front or back, as the case may be).
Subscript a denotes the parameter value for Comfort Mate Foam; subscript b, for Meridian Wave.

2.1. **The wheelchair.** This 2-DOF model is represented by two blocks: one being the seat combined with its cushion of negligible mass, denoted by m_2, and the other, the chair frame (less seat) with tires, denoted by m_1. Since the seat, the pelvis, and chassis & tires (m_1) are interconnected, the biodynamic response of the seat block is dependent upon the transmissibility of the other two blocks through the arrangement of vertical springs (k_2 and k_3) and velocity-dependent dampers (c_2 and c_3) as shown in Figure 1. Between the chassis & tires and ground surface, similar springs and dampers are employed in front and rear pairs with their coefficients denoted by k_{1f}, k_{1r} and c_{1f} and c_{1r} respectively. Table 1 lists the response parameters of the wheelchair as determined by Hikmawan and Nugraha [7], and of the cushions and wheelchair suspension as determined by Garcia-Mendez et al. [6] and Hikmawan and Nugraha [7].

2.2. **The occupant.** The seated figure is treated as a 7-DOF frame emulating the work of Liang and Chiang [13], which employed an idealized anatomy of the human body in seated posture whereby the body parts are isolated at the joints where relative movements are allowed, and the parts considered as lumped masses. The seven blocks, comprising head (m_9), back (m_8), torso (m_7), thorax (m_6), diaphragm (m_5), abdomen (m_4), and pelvis (m_3) are connected by springs and dampers, representing the resilient characteristics of the connective tissues between the components. The parameter values of such human tissues, obtained from various studies of anatomical subsystems [6, 7], are listed in Table 2.

TABLE 2. Parameter values of biodynamic model [13, 26]

Mass [M] (kg)	Damping constant [C] (N/m/sec)	Spring constant [K] (N/m)
$m_3 = 27.7$	$c_3 = 378$	$k_3 = 25500$
$m_4 = 6.02$	$c_4 = 298$	$k_4 = 894.1$
$m_5 = 0.46$	$c_5 = 298$	$k_5 = 894.1$
$m_6 = 1.38$	$c_6 = 298$	$k_6 = 894.1$
$m_7 = 33.33$	$c_7 = 298$	$k_7 = 894.1$
	$c_{78} = 3651$	$k_{78} = 53640$
$m_8 = 6.94$	$c_8 = 3651$	$k_8 = 53640$
$m_9 = 5.5$	$c_9 = 3651$	$k_9 = 53640$

The combined weight of the wheelchair and human body was specified at 99.33 kg. From this model, a set of equations of motion (EOMs) was derived.

3. **Free Body Diagrams of Wheelchair and Seated Figure.** The free body diagram (FBD) associated with the model's 9-DOF is shown in Figure 2. The diagrams represent 9 masses connected by 11 springs and 11 dampers – each of which to be subjected to a force vector, or input excitation. In mechanical terms, these are like springs, dampers and connected masses in the form of lumped parameters making up a wheelchair and occupant system. The FBDs serve as an aid in deducing the force-equilibrium equations for all nine masses.

Consideration of the forces on the nine FBD blocks is limited to acting and reacting vectors according to Newton's Third Law of Motion which states, "for every force acting on a body, there is an equal and opposite reaction" [30]. Hence, with its masses, springs and dampers, the system should give rise to the array of mechanical and reactive forces as shown in Figure 2. Note that the gravitational mass (mg) of any block and its static displacement are not shown in the FBD since the system is assumed to be in a dynamic state from which the force-equilibrium equations are to be deduced.

For example, the FBD of m_1 (chassis & tires) is derived through the following consideration. Between the mass m_1 and ground surface on which the wheelchair is traversing, the tires would exert a stiffness force ($k_{1f}y_0 + k_{1r}y_0$) and a damping force ($c_{1f}y_0 + c_{1r}y_0$) upon the ground. The ground would respond by pushing on the chassis & tires with an equal upward force in the y_0 direction. Due to its inertia, m_1 would resist its positional change. And the tires' stiffness and damping forces are also acting on the ground in the $-y_0$ direction but it is ignored in this study.

4. **Equations of Motion of the Nine DOFs.** The governing EOMs were derived from the FBDs through the application of Newton's Third Law. After mathematical adjustment according to our literature review, the EOMs were transformed into linear

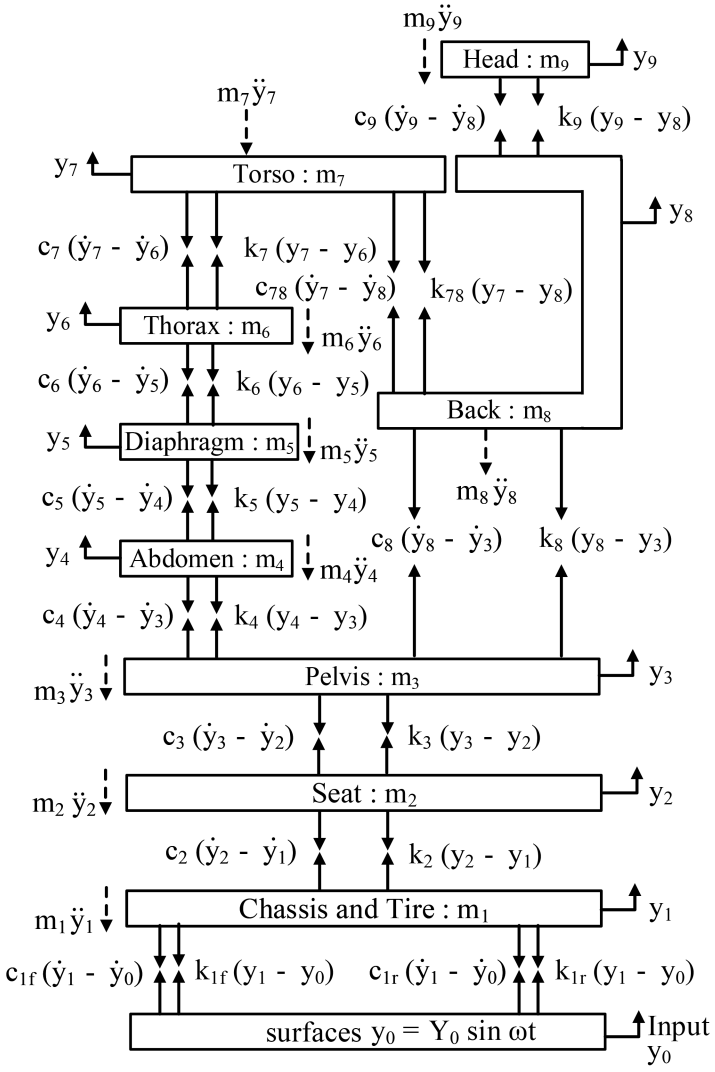

FIGURE 2. Free body diagrams (FBD) of the lumped-parameter model of wheelchair and occupant

polynomials. The model, therefore, was composed of seven isolated segments representing the human body, plus two parts for the wheelchair. These made up nine degrees of freedom requiring nine equations of motion.

The governing EOM for each mass consists of its inertia term and forces exerted on it by the stiffnesses and dampers due to the relative motion of the connected masses. In an EOM, the variables – including m_i, k_i, c_i, y_i, $\dot{y}_i$ and $\ddot{y}_i$, $(i = 1, 2, \ldots, 9)$ – represent the components, i.e., Chassis & Tires, Seat, Pelvis, Abdomen, Diaphragm, Thorax, Torso, Back and Head, respectively. Here y_0 and $\dot{y}_0$ signify the corresponding displacements and velocities upon excitation. The governing second-order linear ordinary differential equations of the nine masses of the composite model (shown in Figure 2) are derived from the FBD by applying the equation of force equilibrium for the human body and wheelchair mass [26, 28]. After mathematical adjustment according to our literature review, the EOMs are transformed into linear polynomials – altogether nine equations to describe the nine DOFs of the model. From the FBDs as shown in Figure 2, the nine EOMs are to be obtained by solving Equations (1) to (9) and expressed as follows:

Wheelchair segment: The Chassis & Tires

$$m_1\ddot{y}_1 + c_2(\dot{y}_1 - \dot{y}_2) + c_{1f}(\dot{y}_1 - \dot{y}_0) + c_{1r}(\dot{y}_1 - \dot{y}_0) + k_{1r}(y_1 - y_0) + k_{1f}(y_1 - y_0) + k_2(y_1 - y_2) = c_{1f}Y_0\omega\cos\omega t + c_{1r}Y_0\omega\cos\omega t + k_{1f}Y_0\sin\omega t + k_{1r}Y_0\sin\omega t, \tag{1}$$

where (i) m_1 is the mass of the chassis & tires, (ii) c_{1f}, k_{1f} and c_{1r}, k_{1r} are, respectively, the damping and spring constant of front tires and rear tires, (iii) $\ddot{y}_1$, $\dot{y}_1$, y_1 refer, respectively, to the acceleration, velocity and displacement of the chassis & tires, (iv) c_2, k_2 and y_2 are, respectively, the damping, spring constant and displacement of the seat, (v) $\dot{y}_0$ and y_0 refer, respectively, to the input velocity and displacement of the tires contact points to the floor. The floor surface will cause the tires to compress, (vi) Y_0, ω are, respectively, the amplitude of input displacement excitation and circular frequency of this displacement applied at the tire contact points to the floor.

Wheelchair segment: The Seat

$$m_2\ddot{y}_2 + c_3(\dot{y}_2 - \dot{y}_3) + c_2(\dot{y}_2 - \dot{y}_1) + k_3(y_2 - y_3) + k_2(y_2 - y_1) = 0, \tag{2}$$

where (i) m_2 is the mass of the seat, (ii) $\ddot{y}_2$, $\dot{y}_2$ refer to the acceleration and velocity of the seat, respectively, (iii) c_3, k_3 are, respectively, the damping and spring constant of the pelvis, (iv) $\dot{y}_3$, y_3 refer to the velocity and displacement of the pelvis, respectively.

Body segment: The Pelvis

$$m_3\ddot{y}_3 + c_4(\dot{y}_3 - \dot{y}_4) + c_3(\dot{y}_3 - \dot{y}_8) + c_8(\dot{y}_3 - \dot{y}_8) + k_4(y_3 - y_4) + k_3(y_3 - y_8) + k_8(y_3 - y_8) = 0, \tag{3}$$

where (i) m_3, $\ddot{y}_3$ are the mass and acceleration of the pelvis, (ii) $\dot{y}_4$, y_4 and $\dot{y}_8$, y_8 refer, respectively, to the velocity and displacement of the abdomen and back, (iii) c_4, k_4 and c_8, k_8 are, respectively, the damping and spring constant of the abdomen and back.

Body segment: The Abdomen

$$m_4\ddot{y}_4 + c_5(\dot{y}_4 - \dot{y}_5) + c_4(\dot{y}_4 - \dot{y}_3) + k_5(y_4 - y_5) + k_4(y_4 - y_3) = 0, \tag{4}$$

where (i) m_4 and $\ddot{y}_4$ are the mass and acceleration of the abdomen, (ii) c_5, k_5 are, respectively, the damping and spring constant of the diaphragm, (iii) $\dot{y}_5$, y_5 refer to the velocity and displacement of the diaphragm, respectively.

Body segment: The Diaphragm

$$m_5\ddot{y}_5 + c_6(\dot{y}_5 - \dot{y}_6) + c_5(\dot{y}_5 - \dot{y}_4) + k_6(y_5 - y_6) + k_5(y_5 - y_4) = 0, \tag{5}$$

where (i) m_5 and $\ddot{y}_5$ are the mass and acceleration of the diaphragm, (ii) c_6, k_6 are, respectively, the damping and spring constant of the thorax, (iii) $\dot{y}_6$, y_6 refer to the velocity and displacement of the thorax, respectively.

Body segment: The Thorax

$$m_6\ddot{y}_6 + c_7(\dot{y}_6 - \dot{y}_7) + c_6(\dot{y}_6 - \dot{y}_5) + k_7(y_6 - y_7) + k_6(y_6 - y_5) = 0, \tag{6}$$

where (i) m_6 and $\ddot{y}_6$ are the mass and acceleration of the thorax, (ii) c_7, k_7 are, respectively, the damping and spring constant of the torso, (iii) $\dot{y}_7$, y_7 refer to the velocity and displacement of the torso, respectively.

Body segment: The Torso

$$m_7\ddot{y}_7 + c_{78}(\dot{y}_7 - \dot{y}_8) + c_7(\dot{y}_7 - \dot{y}_6) + k_{78}(y_7 - y_8) + k_7(y_7 - y_6) = 0, \tag{7}$$

where (i) m_7 and $\ddot{y}_7$ are the mass and acceleration of the torso, (ii) c_{78}, k_{78} are, respectively, the damping and spring constant of tissue between the torso and back, (iii) $\dot{y}_8$, y_8 refer to the velocity, displacement of the back, respectively.

Body segment: The Back

$$m_8\ddot{y}_8 + c_9(\dot{y}_8 - \dot{y}_9) + c_{78}(\dot{y}_8 - \dot{y}_7) + c_8(\dot{y}_8 - \dot{y}_7) + k_9(y_8 - y_9) + k_8(y_8 - y_7) + k_{78}(y_8 - y_7) = 0, \tag{8}$$

where (i) m_8 and $\ddot{y}_8$, are the mass and acceleration of the back, (ii) c_8, k_8 are, respectively, the damping and spring constant of the back, (iii) $\dot{y}_9$, y_9 refer to the velocity and displacement of the head, respectively.

$$\begin{gathered}\text{Body segment: The Head}\\ m_9\ddot{y}_9 + c_9\left(\dot{y}_9 - \dot{y}_8\right) + k_9(y_9 - y_8) = 0,\end{gathered} \tag{9}$$

where (i) m_9 and $\ddot{y}_9$, are the mass and acceleration of the head, (ii) c_9, k_9 are, respectively, the damping and spring constant of the head.

The above nine linear differential equations are solved by computer simulation to yield y_i, $\dot{y}_i$ and $\ddot{y}_i$, $(i = 1, 2, \ldots, 9)$ which are the corresponding displacements, velocities and accelerations, as responses to steady-state sinusoidal forcing functional inputs at different frequencies of vibration. Dividing the amplitude responses of the body parts and wheelchair by the input amplitude of vibration then yield their amplitude ratios. The transmissibility of different seat cushions is then determined over the entire array of body-part responses in the 0.5 to 11 Hz frequency range. The parameters of the body parts and wheelchair, which give maximum vibration responses of the body parts, are listed in Table 2.

5. Nine DOF for Equation System of Motion in Matrix Notation.

5.1. **Model description of the 9-DOF.** The equations related to mass, stiffness and damping are rearranged as algebraic matrices as shown below. Each matrix, upon being multiplied with acceleration, velocity and displacement vectors – all of which being dependent on the characteristics of force – will equal the force vectors of external excitation. All of the equations of motion system with harmonic input excitation for the series/parallel 9-DOF model can be expressed in matrix form as shown in Equations (10) and (11)

$$[M]\{\ddot{y}(t)\} + [C]\{\dot{y}(t)\} + [K]\{y(t)\} = \{F_0\}\sin\omega t, \tag{10}$$

$$\{F_0\} = (c_{1f} + c_{1r})\{\dot{y}_0(t)\} + (k_{1f} + k_{1r})\{y_0(t)\}, \tag{11}$$

where $[M]$, $[C]$ and $[K]$ are 9×9 mass, damping and stiffness matrices, respectively; $\{y(t)\}$, $\{\dot{y}(t)\}$ and $\{\ddot{y}(t)\}$ are displacement, velocity and acceleration vectors of the response system; $\{F_0\}$ is the force vector of the external excitation; $\{y_0(t)\}$ and $\{\dot{y}_0(t)\}$ are displacement and velocity vectors of the external excitation system. Here, $[M]$, $[C]$, $[K]$, $\{y(t)\}$, $\{\dot{y}(t)\}$, $\{\ddot{y}(t)\}$, $\{y_0(t)\}$, $\{\dot{y}_0(t)\}$ and $\{F_0\}$ are written as

$$[M] = \begin{bmatrix} m_1 & 0 & 0 & 0 & 0 & 0 & 0 & 0 & 0 \\ 0 & m_2 & 0 & 0 & 0 & 0 & 0 & 0 & 0 \\ 0 & 0 & m_3 & 0 & 0 & 0 & 0 & 0 & 0 \\ 0 & 0 & 0 & m_4 & 0 & 0 & 0 & 0 & 0 \\ 0 & 0 & 0 & 0 & m_5 & 0 & 0 & 0 & 0 \\ 0 & 0 & 0 & 0 & 0 & m_6 & 0 & 0 & 0 \\ 0 & 0 & 0 & 0 & 0 & 0 & m_7 & 0 & 0 \\ 0 & 0 & 0 & 0 & 0 & 0 & 0 & m_8 & 0 \\ 0 & 0 & 0 & 0 & 0 & 0 & 0 & 0 & m_9 \end{bmatrix} \tag{12}$$

$$[C] = \begin{bmatrix} c_2+c_{1f}+c_{1r} & -c_2 & 0 & 0 & 0 & 0 & 0 & 0 & 0 \\ -c_2 & c_3+c_2 & -c_3 & 0 & 0 & 0 & 0 & 0 & 0 \\ 0 & -c_3 & c_3+c_4+c_8 & -c_4 & 0 & 0 & 0 & -c_8 & 0 \\ 0 & 0 & -c_4 & c_4+c_5 & -c_5 & 0 & 0 & 0 & 0 \\ 0 & 0 & 0 & -c_5 & c_5+c_6 & -c_6 & 0 & 0 & 0 \\ 0 & 0 & 0 & 0 & -c_6 & c_6+c_7 & -c_7 & 0 & 0 \\ 0 & 0 & 0 & 0 & 0 & -c_7 & c_7+c_{78} & -c_{78} & 0 \\ 0 & 0 & -c_8 & 0 & 0 & 0 & -c_{78} & c_8+c_{78}+c_9 & -c_9 \\ 0 & 0 & 0 & 0 & 0 & 0 & 0 & -c_9 & c_9 \end{bmatrix} \tag{13}$$

$$[K] = \begin{bmatrix} k_2+k_{1f}+k_{1r} & -k_2 & 0 & 0 & 0 & 0 & 0 & 0 & 0 \\ -k_2 & k_3+k_2 & -k_3 & 0 & 0 & 0 & 0 & 0 & 0 \\ 0 & -k_3 & k_3+k_4+k_8 & -k_4 & 0 & 0 & 0 & -k_8 & 0 \\ 0 & 0 & -k_4 & k_4+k_5 & -k_5 & 0 & 0 & 0 & 0 \\ 0 & 0 & 0 & -k_5 & k_5+k_6 & -k_6 & 0 & 0 & 0 \\ 0 & 0 & 0 & 0 & -k_6 & k_6+k_7 & -k_7 & 0 & 0 \\ 0 & 0 & 0 & 0 & 0 & -k_7 & k_7+k_{78} & -k_{78} & 0 \\ 0 & 0 & -k_8 & 0 & 0 & 0 & -k_{78} & k_8+k_{78}+k_9 & -k_9 \\ 0 & 0 & 0 & 0 & 0 & 0 & 0 & -k_9 & k_9 \end{bmatrix} \tag{14}$$

$$\{y(t)\} = \begin{Bmatrix} y_1 & y_2 & y_3 & y_4 & y_5 & y_6 & y_7 & y_8 & y_9 \end{Bmatrix}^T, \tag{15}$$

$$\{\dot{y}(t)\} = \begin{Bmatrix} \dot{y}_1 & \dot{y}_2 & \dot{y}_3 & \dot{y}_4 & \dot{y}_5 & \dot{y}_6 & \dot{y}_7 & \dot{y}_8 & \dot{y}_9 \end{Bmatrix}^T, \tag{16}$$

$$\{\ddot{y}(t)\} = \begin{Bmatrix} \ddot{y}_1 & \ddot{y}_2 & \ddot{y}_3 & \ddot{y}_4 & \ddot{y}_5 & \ddot{y}_6 & \ddot{y}_7 & \ddot{y}_8 & \ddot{y}_9 \end{Bmatrix}^T, \tag{17}$$

$$\{F_0\} = \begin{Bmatrix} c_0\dot{y}_0 + k_0 y_0 & 0 & 0 & 0 & 0 & 0 & 0 & 0 & 0 \end{Bmatrix}^T, \tag{18}$$

$$\{\dot{y}_0(t)\} = \begin{Bmatrix} \dot{y}_0 & 0 & 0 & 0 & 0 & 0 & 0 & 0 & 0 \end{Bmatrix}^T, \tag{19}$$

$$\{y_0(t)\} = \begin{Bmatrix} y_0 & 0 & 0 & 0 & 0 & 0 & 0 & 0 & 0 \end{Bmatrix}^T, \tag{20}$$

$$k_0 = k_{1f} + k_{1r}, \tag{21}$$

$$c_0 = c_{1f} + c_{1r}. \tag{22}$$

5.2. **Frequency response analysis.** The frequency response function is analyzed using Euler's formula

$$e^{j\omega t} = \cos\omega t + j\sin\omega t. \tag{23}$$

Euler's formula offers the agility in dealing with the real and imaginary parts of the input as well as those of the output – a capability that aided in solving the complex equations of motion. When the linear equation of motion is expressed as Equation (10), we have only the imaginary part in complex exponential form which is $\{F_0\}(\sin\omega t) = \Im[\{F_0\}e^{j\omega t}]$. Therefore, when $\Im[\{F_0\}e^{j\omega t}]$ as a function of time is substituted in Equation (10), we obtained

$$[M]\{\ddot{y}(t)\} + [C]\{\dot{y}(t)\} + [K]\{y(t)\} = \{F_0\}e^{j\omega t}, \tag{24}$$

where $\{F_0\}$ represents the magnitude of input force excitation vector, while $e^{j\omega t}$ a complex exponential term.

5.2.1. *Exponential function vectors of the excitation.* The derivatives of equation of excitation from the base state are given by

$$\begin{cases} \{y_0(t)\} = \{Y_0\}\, e^{j\omega t} \\ \{\dot{y_0}(t)\} = j\omega\, \{Y_0\}\, e^{j\omega t} \end{cases}, \tag{25}$$

where $\{Y_0\}$ represents the magnitude of input displacement excitation vector.

5.2.2. *Exponential function vectors of the response.* The derivatives of equation of response to vibrations are given by

$$\begin{cases} \{y(t)\} = \{Y\}e^{j\omega t} \\ \{\dot{y}(t)\} = j\omega\{Y\}e^{j\omega t} \\ \{\ddot{y}(t)\} = -\omega^2\{Y\}e^{j\omega t} \end{cases}, \tag{26}$$

where $\{Y\}$ represents the magnitude of displacement response vector.

5.2.3. *Exponential function vectors of MDOF.* Input force excitation vectors on the wheelchair are expressed by

$$\{F_0\}e^{j\omega t} = (c_{1f} + c_{1r})\{Y_0\}j\omega e^{j\omega t} + (k_{1f} + k_{1r})\{Y_0\}e^{j\omega t}, \tag{27}$$

where c_{1f}, k_{1f} and c_{1r}, k_{1r} are the damping and spring constants of front tires and rear tires, respectively, upon substituting $y_0(t)$, $\dot{y_0}(t)$, $y(t)$, $\dot{y}(t)$, $\ddot{y}(t)$ of (25), (26) and (27) are substituted in Equation (24), and the equation for MODF system is obtained as

$$\left[-\omega^2[M] + j\omega[C] + [K]\right]\{Y\}e^{j\omega t} = \{F_0\}e^{j\omega t}. \tag{28}$$

5.3. **Analysis of 9DOF system of complex function using transfer function.** Equations of motion of the 9DOF system are substituted of the complex function in the transfer function (expressed in hertz) in Equation (28). Further manipulation of this equation enables us to eliminate the time-dependent part, thereby yielding the algebraic equation

$$\frac{\{Y(j\omega)\}}{\{F_0(j\omega)\}} = \frac{1}{[-\omega^2[M] + j\omega[C] + [K]]} = [Q(j\omega)], \tag{29}$$

where $[Q(j\omega)]$ is the impedance matrix of a complex matrix combination of the mass and stiffness matrices.

5.3.1. *Solution of impedance matrix.* Next, we examine Equation (29). The $[Q(j\omega)]$ term therein is a matrix of impedance for assessing mechanical responses from the human and vehicle frames, and is expressed in transfer function matrices as

$$[Q(j\omega)] = [K] + j\omega[C] - \omega^2[M], \tag{30}$$

where

$$\begin{cases} q_{11} = k_{11} + j\omega c_{11} - \omega^2 m_{11} \\ q_{12} = k_{12} + j\omega c_{12} - \omega^2 m_{12} \\ q_{13} = k_{13} + j\omega c_{13} - \omega^2 m_{13} \\ \qquad\qquad \vdots \\ q_{99} = k_{99} + j\omega c_{99} - \omega^2 m_{99} \end{cases}, \tag{31}$$

$$q_{ij}(j\omega) \;=\; \sum_{i=1}^{n}\sum_{j=1}^{n} k_{ij} + j\omega c_{ij} - \omega^2 m_{ij} \;\; (i, j = 1, 2, \ldots, 9) \tag{32}$$

and

$$[Q(j\omega)] = \begin{bmatrix} q_{11} & q_{12} & q_{13} & q_{14} & q_{15} & q_{16} & q_{17} & q_{18} & q_{19} \\ q_{21} & q_{22} & q_{23} & q_{24} & q_{25} & q_{26} & q_{27} & q_{28} & q_{29} \\ q_{31} & q_{32} & q_{33} & q_{34} & q_{35} & q_{36} & q_{37} & q_{38} & q_{39} \\ \vdots & \vdots & \vdots & \vdots & \vdots & \vdots & \vdots & \vdots & \vdots \\ q_{91} & q_{92} & q_{93} & q_{94} & q_{95} & q_{96} & q_{97} & q_{98} & q_{99} \end{bmatrix}.$$

5.3.2. *Displacement responses by transfer function matrix.* $\{Y(j\omega)\}$ and $\{F_0(j\omega)\}$ are the corresponding complex Fourier transform vectors of $\{y_i(j\omega)\}$ and $\{F_i(j\omega)\}$ respectively and ω, the excitation frequency. The $\{Y(j\omega)\}$ portion, which contains complex displacement responses from the nine mass segments, is represented by $\{Y(j\omega)\} = \{y_1(j\omega), y_2(j\omega), y_3(j\omega), \ldots, y_9(j\omega)\}$. Upon substitution in Equation (28), we obtain

$$\begin{cases} [Q(j\omega)]\{Y(j\omega)\} = \{F_0(j\omega)\} \\ \{Y(j\omega)\} = \{F_0(j\omega)\}[Q(j\omega)]^{-1} \end{cases}, \tag{33}$$

where

$$[Q(j\omega)]^{-1} = [H(j\omega)] = \begin{bmatrix} H_{11} & H_{12} & H_{13} & H_{14} & H_{15} & H_{16} & H_{17} & H_{18} & H_{19} \\ H_{21} & H_{22} & H_{23} & H_{24} & H_{25} & H_{26} & H_{27} & H_{28} & H_{29} \\ H_{31} & H_{32} & H_{33} & H_{34} & H_{35} & H_{36} & H_{37} & H_{38} & H_{39} \\ \vdots & \vdots & \vdots & \vdots & \vdots & \vdots & \vdots & \vdots & \vdots \\ H_{91} & H_{92} & H_{93} & H_{94} & H_{95} & H_{96} & H_{97} & H_{98} & H_{99} \end{bmatrix} \tag{34}$$

and $H_{ij}(j\omega)$ is response at i due to a harmonic excitation at j. The $[Q(j\omega)]$ had been generated by the equations of mass, damping and stiffness matrices. Its inverse, as shown in (34), became a transfer function matrix which is $[H(j\omega)]$. This gives us the set of matrix equations

$$\begin{Bmatrix} y_1(j\omega) \\ y_2(j\omega) \\ y_3(j\omega) \\ \vdots \\ y_9(j\omega) \end{Bmatrix} = \begin{bmatrix} H_{11} & H_{12} & H_{13} & H_{14} & H_{15} & H_{16} & H_{17} & H_{18} & H_{19} \\ H_{21} & H_{22} & H_{23} & H_{24} & H_{25} & H_{26} & H_{27} & H_{28} & H_{29} \\ H_{31} & H_{32} & H_{33} & H_{34} & H_{35} & H_{36} & H_{37} & H_{38} & H_{39} \\ \vdots & \vdots & \vdots & \vdots & \vdots & \vdots & \vdots & \vdots & \vdots \\ H_{91} & H_{92} & H_{93} & H_{94} & H_{95} & H_{96} & H_{97} & H_{98} & H_{99} \end{bmatrix} \begin{Bmatrix} F_1(j\omega) \\ F_2(j\omega) \\ F_3(j\omega) \\ \vdots \\ F_9(j\omega) \end{Bmatrix}, \tag{35}$$

where $\{y_i(j\omega)\}$ and $\{F_i(j\omega)\}$, $(i = 1, 2, \ldots, 9)$ are complex displacement responses and complex excitation forces on the mass segments from body and wheelchair $m_i(j\omega)$, $(i = 1, 2, \ldots, 9)$ as a function of ω, respectively. By using $y_i(j\omega)$, $(i = 1, 2, \ldots, 9)$ in (35) to determine the outputted displacement vectors from the EOM, and setting the input force excitation vectors $F_i(j\omega)$, $(i = 2, \ldots, 9) = 0$; we obtain the displacement values of each DOF of the body segments and wheelchair components as

$$\begin{cases} y_1(j\omega) = H_{11}(j\omega)F_1(j\omega) \\ y_2(j\omega) = H_{21}(j\omega)F_1(j\omega) \\ y_3(j\omega) = H_{31}(j\omega)F_1(j\omega) \\ \qquad\qquad \vdots \\ y_9(j\omega) = H_{91}(j\omega)F_1(j\omega) \end{cases}. \tag{36}$$

5.4. **Transmissibility of response versus excitation.** Transmissibility is the complex ratio of the magnitude of displacement response from a system under steady-state forced vibration to the magnitude of excitation, all at a given frequency range. The ratio defines the input vibration being transmitted to the wheelchair occupant. Transmissibility (TR) is defined as output response divided by input excitation [6, 13].

$$TR = \frac{|y_i(j\omega)|}{|y_0(j\omega)|} \quad (i = 1, 2, \ldots, 9). \tag{37}$$

In Equation (37), $|y_i(j\omega)|$ $(i = 1, 2, \ldots, 9)$ represent the magnitudes of displacement responses on the mass segments from Chassis & Tires (m_1), Seat (m_2), Pelvis (m_3), Abdomen (m_4), Diaphragm (m_5), Thorax (m_6), Torso (m_7), Back (m_8) and Head (m_9), and $|y_0(j\omega)|$ represents the magnitude of input displacement excitation. Therefore, Equation (37) shows the ratio of output response to input excitation [1, 9]. Human body and vehicle responses to excitation are assessed in terms of biodynamic response functions. A transfer function, itself being a biodynamic response function, is also known as vibration transmissibility. Displacement responses are calculated for all body segments using the transfer functions.

6. **Numerical Example.** The coupled linear differential equations from (1) to (10) are solved by using Euler's formula (23) along with a procedure according to Equations (24) to (36) in order to obtain the $y_i(j\omega)$ $(i = 1, 2, \ldots, 9)$ response to steady state, sinusoidal, forcing inputs to the tires at different vibration frequencies. The magnitude ratios of forces acting on various body and wheelchair components are obtained by working out the magnitude of output displacements of the components relative to the amplitudes of input excitation (Y_0, at the wheelchair tires). The range of parameters for the suspension of the occupied wheelchair is selected so as to confine the responses from the human body segments within the frequency range between 0.5 Hz and 20 Hz [6]. These parameters and their values are listed in Tables 1 and 2.

6.1. **Validation of the occupant and wheelchair model.** Acceleration ratios of the input forces acting on the occupant from head to pelvis were plotted as acceleration ratios versus input frequency. At the 0.5 to 11 Hz frequency range, the obtained ratios had their lowest values [26]. Tables 1 and 2 list the values of parameters for stiffness and damping applicable to the tested Comfort Mate Foam and Meridian Wave seat cushions. Figure 3 shows the results of acceleration or displacement ratios obtained from our model according to the input parameters listed in the tables. The first peak value occurs at approximately frequency of 3 to 4 Hz. Superimposed thereon is the experimental curve derived by Patil and Palanichamy, from tests using sinusoidal inputs [21, 26]. Since good agreement between the curves was apparent, we may conclude that our composite model is of acceptable quality.

6.2. **Transmissibility of the occupant and wheelchair model.** The transfer function that was employed to solve this linear system was taken from $y_0(j\omega)$ with maximum magnitudes under different seat cushions. Transmissibility values were determined for tests on Comfort Mate Foam and Meridian Wave cushions having the parameters K and C as shown in Table 2. Note that Comfort Mate Foam is a foam-based cushion; while Meridian Wave, an air-based one. The resulting TR magnitudes resulting from input excitation to occupant's head and pelvis for the two cushion types are shown in Figure 4. Note that tests with Meridian Wave cushion gave rise to a peak TR of 4.38 at frequency 2 Hz, which is in close proximity with those from Comfort Mate Foam, which rose to 3.88 at frequency 2.1 Hz. The solid line (and its upper and lower limits) in the graphs defines

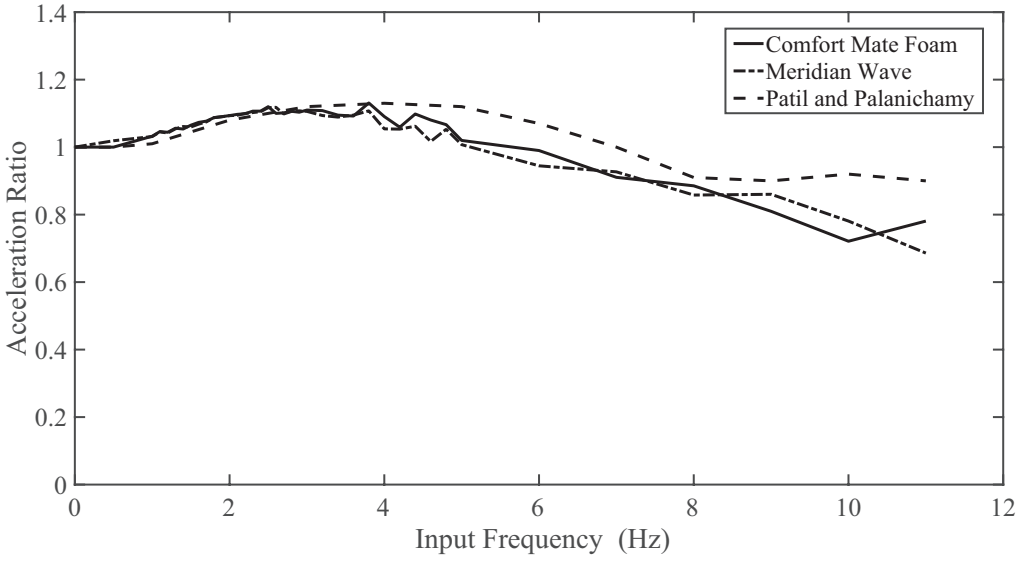

FIGURE 3. Comparison of acceleration ratios on wheelchair from excitation to occupant head for tests on two seat cushion types: Comfort Mate Foam and Meridian Wave

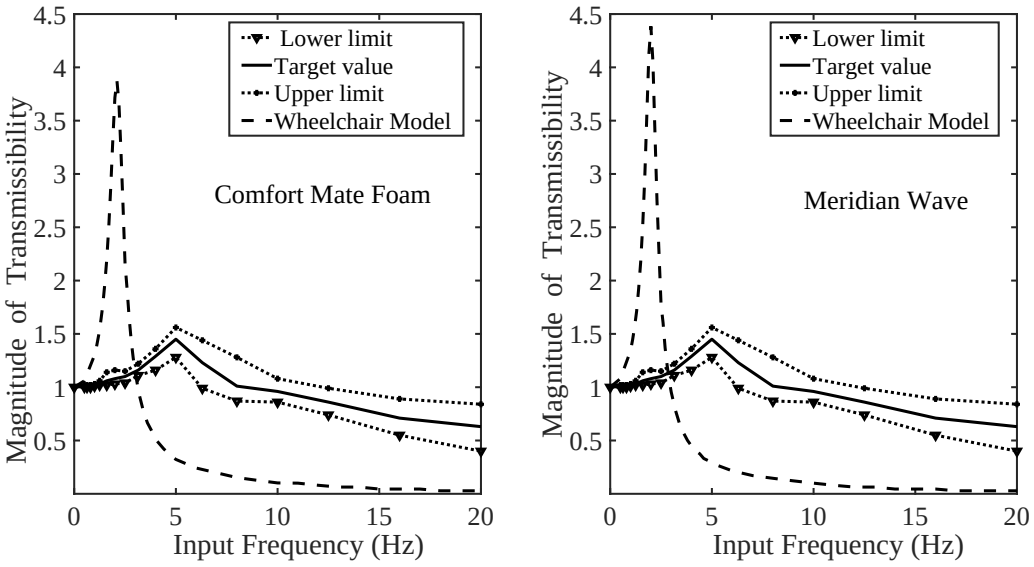

FIGURE 4. Comparison of vibration transmissibility from excitation to wheelchair occupant's head for tests on two seat cushion types: Comfort Mate Foam and Meridian Wave

the target values representing the comfort and health safety boundary of transmissibility below which vibrations should be confined [13]. The target values are outcomes of tests by Liang et al. [13, 14] which yield the apexes of the curves occurring at 5.1 Hz for seat-to-head transmissibility when comparison is made with different seat cushions on standard wheelchairs.

For solutions that describe the behavior of a mass (m_1 to m_9) per unit input force as a function of frequency, y_1 to y_9 are the resulting displacements or magnitudes of model response, while y_0 the displacement which is the base magnitude of excitation. Upon examination of the transmissibility curves obtained from model runs for all nine cases –

head, back, torso, and so on – and the resulting TR values between the cases of Comfort Mate Foam and Meridiam Wave cushions, it was found that the former cushion produced a lower TR. Note that between the two brands, Comfort Mate Foam has larger spring stiffness constants.

Figures 5 to 8, which plot transmissibility versus input frequency, are employed for investigating the effects of vibration on the model's head. In Figure 5, the maximum TR in the case of Comfort Mate Foam cushion is found to have a lower value than that of the Meridian Wave. TR values are computed by taking the magnitudes of $y_3(j\omega)$ to $y_9(j\omega)$

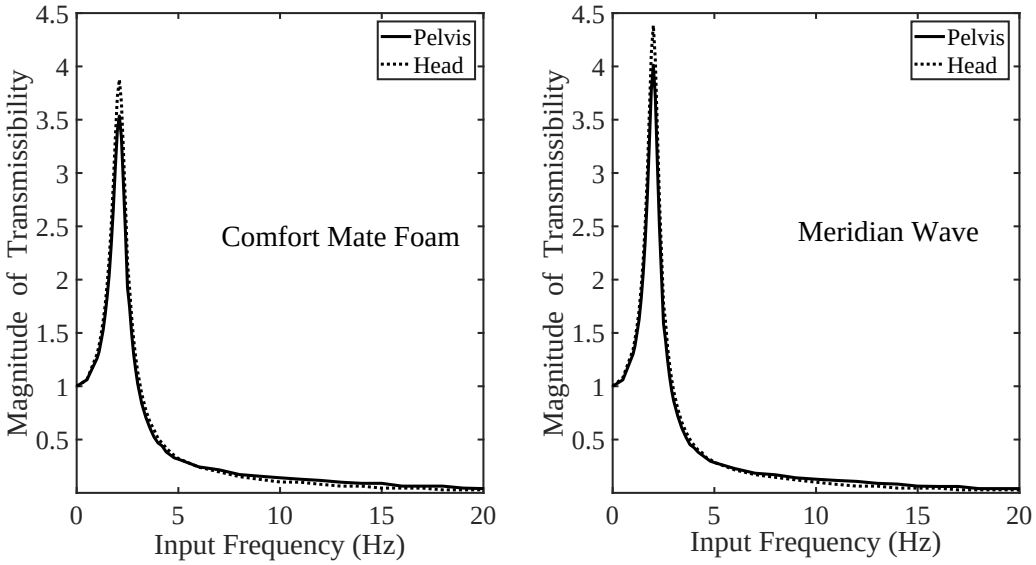

FIGURE 5. Comparison of vibration transmissibility from excitation to wheelchair occupant's head and pelvis for tests on two seat cushion types: Comfort Mate Foam and Meridian Wave

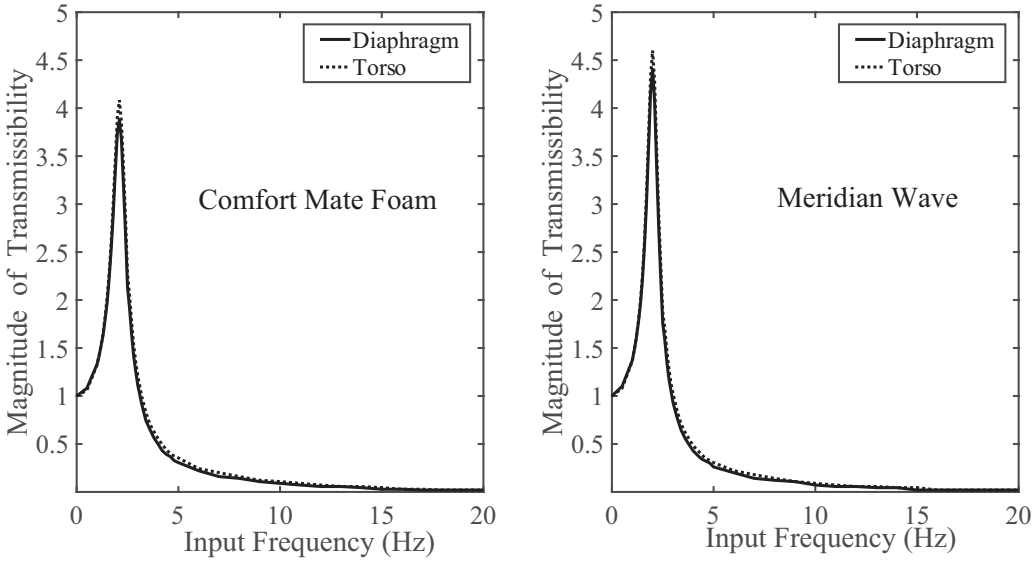

FIGURE 6. Comparison of transmissibility from excitation to chair occupant's diaphragm and torso, for tests on two seat cushion types: Comfort Mate Foam and Meridian Wave

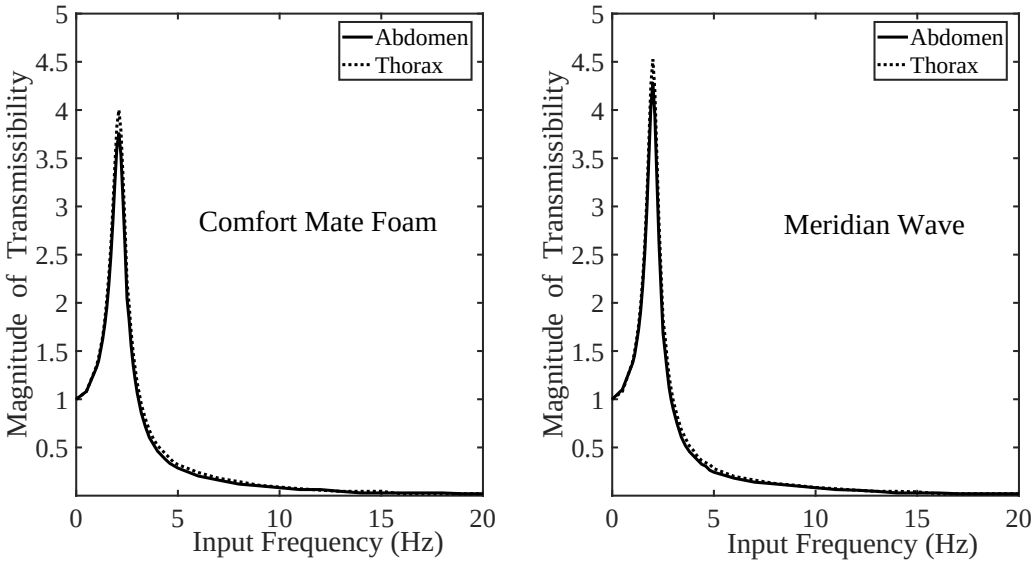

FIGURE 7. Comparison of transmissibility from excitation to chair occupant's abdomen and thorax, for tests on two seat cushion types: Comfort Mate Foam and Meridian Wave

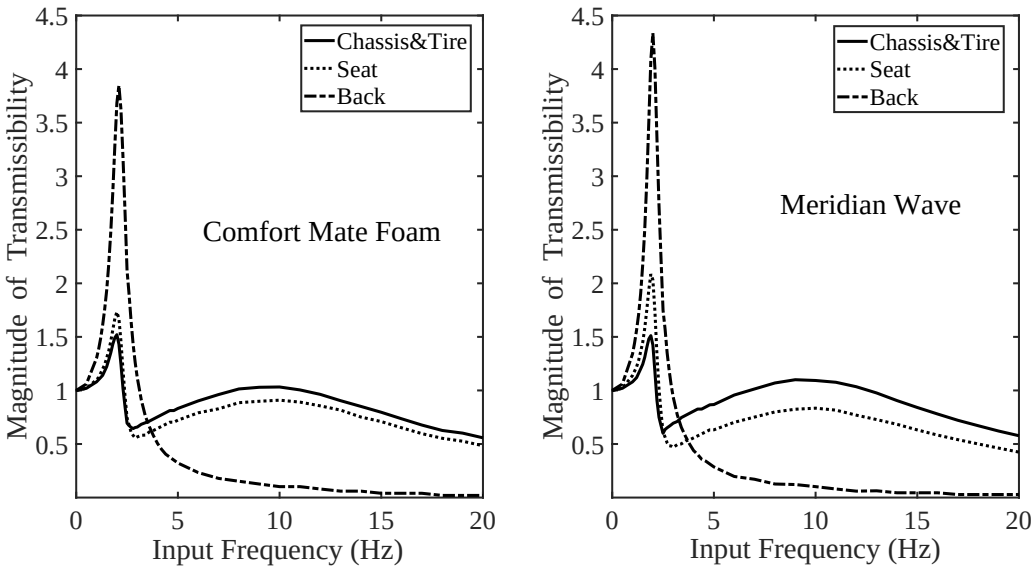

FIGURE 8. Comparison of transmissibility from excitation to occupant's back, wheelchair seat and Chassis & Tires, for tests on two cushion types: Comfort Mate Foam and Meridian Wave

(the response of body segments to excitation) and dividing them with $y_0(j\omega)$, which is the input displacement excitation. If we increase the stiffness constant, the magnitude of TR will decrease, but the related position of frequency will increase as well due to the change in natural frequency of the system.

The maximum TR for the body segments is examined in tests on the two cushion types, which yielded very similar responses in both scenarios. The torso is the most responsive, while the pelvis, the least. In particular, maximum TR in the case of Comfort Mate Foam occurred at 2.1 Hz, whereas that for Meridian Wave occurred a tad lower, at 2 Hz [6].

Responses of the head and seat cushions were examined against the health safe limits, as shown in Figure 4, for tests with the two seat cushion types. In the case of Comfort Mate foam, the responses of the body parts showed transmissibility magnitudes higher than the target line when the input frequency was in the range 0.5 to 3.6 Hz, and below the target line when the input frequency exceeded 3.7 Hz. Similarly, with the Meridian Wave, the transmissibility magnitudes were above the target line when input frequency was between 0.5 to 3.5 Hz, and fell below it when input frequency was increased beyond 3.6 Hz.

The chassis & tires, in tests with the two cushion types, yielded very similar responses to vibrations. Upon comparing the separate performances of the two cushion types, however, the Comfort Mate Foam was seen to yield a lower value of transmissibility which occurred at a lower input frequency than those of the Meridian Wave. From the vast improvement on model responses as seen in this study, it is therefore recommended that cushion parameters be included in the future engineering of wheelchair seat in order to provide better riding comfort [18, 19].

The insights gained from evaluation of the model in this case will help in understanding the behavior of vibration. The investigation was essentially a study in applied dynamics with the input excitation producing an effect equivalent to vibrating harmonics on the wheelchair. In a real-life situation, excitation originates from the floor, spreads to and subjects the wheelchair in vibration. The fundamental approach to reducing such vibration on the wheelchair has the following steps: i) change the properties of the system; ii) change its natural frequency and iii) adjust its damper setup [24, 25].

Regular device monitoring is required for a proper maintenance routine, and when necessary, the device should be taken out of use or repairs administered. A simple solution worth considering is changing or adding a suitable seat cushion, which generally could be carried out without incurring too high a cost.

7. **Conclusions.** The composite model for this study is that of a wheelchair and an occupant in upright sitting posture without backrest support, simulated as a 9-DOF integrated human-vehicle system, to be operated in steady-state equilibrium under sinusoidal excitation. The model is described by nine linear differential equations which are mathematically transformed into nine EOMs. Output responses of the model to excitation input are obtained in terms of acceleration ratios and displacement transmissibility ratios (TR); and these are compared with similar results cited in industry literature in order to validate the model. TRs of the component masses (blocks) can be computed for each individual DOF over the range of input frequencies. This method thus allows the comparison of the peak TR values of the DOFs as a function of input frequencies. Results of this study indicated that as the input frequency approached the high side, both cushions exhibited more intense TRs than did the body parts. On the low side of input frequency, the converse was found, i.e., the body parts produced higher TRs than did the cushions.

The modelling approach of this study should be useful for practitioners of wheelchair seat design in helping to investigate the behavior of harmful vibrations. The next level of research in this area may be in building stronger models, supplanting the current linear system with non-linear equations, that should give more sophisticated prediction of vibration behavior for the refinement of the cushion's shock absorption properties.

Acknowledgment. This work was partially supported by JSPS KAKENHI Grant Number JP21K03930.

REFERENCES

[1] S. Maeda, M. Futatsuka, J. Yonesaki and M. Ikeda, Relationship between questionnaire survey results of vibration complaints of wheelchair users and vibration transmissibility of manual wheelchair, *Environmental Health and Preventive Medicine*, vol.8, no.3, pp.82-89, 2003.

[2] J. Wu and Y. Qiu, Modelling of seated human body exposed to combined vertical, lateral and roll vibrations, *Journal of Sound and Vibration*, vol.485, DOI: 10.1016/j.jsv.2020.115509, 2020.

[3] K. Yamada, Y. Zhao, S. Shiomi, T. Suzuki, D. T. Nguyen, T. Noguchi and K. Chamnongthait, Estimation of anxiety at utilizing wheelchair by measuring brain waves in the case of going down slopes using wheelchair, *The 13th International Conference on Electrical Engineering/Electronics, Computer, Telecommunications and Information Technology*, 2016.

[4] W. Budiharto, Intelligent controller of electric wheelchair from manual wheelchair for disabled person using 3-axis joystick, *ICIC Express Letters, Part B: Applications*, vol.12, no.2, pp.201-206, 2021.

[5] M. Mano and G. Capi, An adaptive BMI based method for real-time wheelchair navigation, *International Journal of Innovative Computing, Information and Control*, vol.9, no.12, pp.4963-4972, 2013.

[6] Y. Garcia-Mendez, J. L. Pearlman, R. A. Cooper and M. L. Boninger, Dynamic stiffness and transmissibility of commercially available wheelchair cushions using a laboratory test method, *Journal of Rehabilitation Research & Development*, vol.49, no.1, pp.7-22, 2012.

[7] M. F. Hikmawan and A. S. Nugraha, Analysis of electric wheelchair passenger comfort with a half-car model approach, *2016 International Conference on Sustainable Energy Engineering and Application (ICSEEA)*, pp.76-80, 2016.

[8] Y. Matsuoka, K. Kawai and R. Sato, Vibration simulation model of passenger-wheelchair system in wheelchair-accessible vehicle, *Journal of Mechanical Design*, vol.125, pp.779-785, 2003.

[9] T. H. Kim, Y. T. Kim and Y. S. Yoon, Development of a biomechanical model of the human body in a sitting posture with vibration transmissibility in the vertical direction, *Int. J. Ind. Ergon.*, vol.35, no.9, pp.817-829, 2006.

[10] ISO 2631-1, *Mechanical Vibration and Shock – Evaluation of Human Exposure to Whole-Body Vibration – Part 1: General Requirements*, International Organization for Standardization, Geneva, 1997.

[11] A. Sezgin and Y. Z. Arslan, Analysis of the vertical vibration effects on ride comfort of vehicle driver, *Journal of Vibroengineering*, vol.14, no.2, pp.559-571, 2012.

[12] Y. Wan and J. M. Schimmels, Improved vibration isolating seat suspension designs based on position-dependent nonlinear stiffness and damping characteristics, *Journal of Dynamic Systems Measurement and Control*, vol.125, no.3, pp.330-338, 2003.

[13] C. C. Liang and C. F. Chiang, A study on biodynamic models of seated human subjects exposed to vertical vibration, *Int. J. Ind. Ergon.*, vol.36, no.10, pp.869-890, 2006.

[14] C. C. Liang, C. F. Chiang and T. G. Nguyen, Biodynamic responses of seated pregnant subjects exposed to vertical vibrations in driving conditions, *Vehicle Syst. Dyn.*, vol.45, pp.1017-1049, 2007.

[15] G. A. Hassaan, Car dynamics using quarter model and passive suspension, Part V: Frequency response considering driver-seat, *International Journal of Scientific Research Engineering & Technology*, vol.4, no.4, pp.357-365, 2015.

[16] P. É. Boileau and S. Rakheja, Whole-body vertical biodynamic response characteristics of the seated vehicle driver: Measurement and model development, *Int. J. Ind. Ergon.*, vol.22, no.6, pp.449-472, 1998.

[17] P. S. Requejo, G. Kerdanyan, J. Minkel, R. Adkins and R. Waters, Effect of rear suspension and speed on seat forces and head accelerations experienced by manual wheelchair riders with spinal cord injury, *Journal of Rehabilitation Research and Development*, vol.45, no.7, pp.985-996, 2008.

[18] H. T. Bui, L. V. Nguyen, K. Debray, Q.-B. Tao and P. Lestriez, Modeling and experimental of the mechanical behavior of seat cushion for wheelchair users, *IOP Conference Series: Materials Science and Engineering*, pp.1-8, 2019.

[19] Y. A. Wicaksono, L. Herdiman and S. Susmartini, Cushion seat design on manual wheelchair for people with paralysis using value engineering method to improve activity comfort: A preliminary study, *Journal of Physics: Conference Series*, vol.1450, no.1, pp.1-9, 2020.

[20] J. W. Chow and C. E. Levy, Wheelchair propulsion biomechanics and wheelers' quality of life: An exploratory review, *Disability and Rehabilitation: Assistive Technology*, vol.6, no.5, pp.365-377, 2011.

[21] T. Yoshimura, K. Nakai and G. Tamaoki, Multi-body dynamics modelling of seated human body under exposure to whole-body vibration, *Industrial Health*, vol.43, no.3, pp.441-447, 2005.

[22] C. P. DiGiovine, R. A. Cooper, S. G. Fitzgerald, M. L. Boninger, E. J. Wolf and S. Guo, Whole-body vibration during manual wheelchair propulsion with selected seat cushions and back supports, *IEEE Trans. Neural Systems and Rehabilitation Engineering*, vol.11, no.3, pp.311-322, 2003.
[23] G. A. Hassaan and N. Mohammed, Frequency response of 10 degrees of freedom full-car model for ride comfort, *International Journal of Scientific Research Engineering*, vol.4, no.1, pp.43-49, 2015.
[24] Z. Dziechciowski and M. Kromka-Szydek, Vibration transmitted to the human body during the patient's ride in a wheelchair, *Archives of Acoustics*, vol.42, no.1, pp.137-148, 2017.
[25] O. Lariviere, D. Chadefaux, C. Sauret and P. Thoreux, Vibration transmission during manual wheelchair propulsion: A systematic review, *Vibration*, vol.4, pp.444-481, 2021.
[26] M. K. Patil and M. S. Palanichamy, A mathematical model of tractor-occupant system with a new seat suspension for minimization of vibration response, *Applied Mathematical Modelling*, vol.12, pp.63-71, 1988.
[27] P. Kumbhar, P. Xu and J. Yang, Evaluation of human body response for different vehicle seats using a multibody biodynamic model, *IEEE SAE Technical Paper*, pp.1-14, 2013.
[28] J. D. Quadros, P. Suhas and N. L. Vaishak, A numerical study for determining the ideal operating speed for a two-wheeler rider on varying terrain amplitudes, *J. Mech. Sci. Technol.*, vol.30, pp.2435-2442, 2016.
[29] Y. Cho and Y. S. Yoon, Biomechanical model of human on seat with backrest for evaluating ride quality, *Int. J. Ind. Ergon.*, vol.27, no.5, pp.331-345, 2001.
[30] P. Cornille, Review of the application of Newton's Third Law in physics, *Progress in Energy and Combustion Science*, vol.25, pp.161-210, 1998.

Author Biography

Pongtep Weerapong received the B.E. degree in Materials Engineering, 2005; the M.E. degree in Polymer Processing Engineering, 2007 from King Mongkut's University of Technology Thonburi (KMUTT), Thailand.

Pongtep is currently a doctoral candidate in Mechanical Science and Technology at Gunma University, Japan. His research interests include assistive technology for children with disabilities and whole-body vibration.

Kotaro Hashikura received the B.S. degree in Mechanical Engineering from Kyushu Institute of Technology, Fukuoka, Japan, 2006; the M.S. degree of Informatics from Kyoto University, Kyoto, Japan, 2010, and the Doctor Degree in Engineering from Tokyo Metropolitan University, Tokyo, Japan, 2014. From 2014 until 2018, he had been a Project Research Associate at the Faculty of System Design, Tokyo Metropolitan University.

Asst. Prof. Hashikura is currently a full-time professor at Division of Mechanical Science and Technology, Gunma University, Japan. His research interests include time-delay-related control techniques, such as deadbeat, preview-prediction and repetitive controls. He is a member of IEEE, ISCIE and SICE.

Md Abdus Samad Kamal received the B.Sc. degree in Electrical and Electronic Engineering from Khulna University of Engineering and Technology (KUET), Khulna, Bangladesh in 1997; Master and Doctor degrees from Kyushu University from Graduate School of Information Science and Electrical Engineering, Japan in 2003 and 2006, respectively. He was a post-doctoral fellow in Kyushu University till November 2006.

Assoc. Prof. Kamal is currently a full-time professor at Division of Mechanical Science and Technology, Gunma University, Japan. His current research interests are reinforcement learning, intelligent transportation systems, and multiagent systems. He is a member of IEEE and SICE.

Kou Yamada received B.S. and M.S. degrees in Electrical and Information Engineering from Yamagata University, Yamagata, Japan, 1987 and 1989, respectively; and the Dr. Eng. Degree from Osaka University, Osaka, Japan in 1997.

Prof. Yamada is currently a full-time professor at Division of Mechanical Science and Technology, Gunma University, Japan. His research interests include robust control, repetitive control, process control and control theory for inverse systems and infinite-dimensional systems. Dr. Yamada received the 2005 Yokoyama Award in Science and Technology, the 2005 Electrical Engineering/Electronics, Computer, Telecommunication, and Information Technology International Conference (ECTI-CON2005) Best Paper Award, the Japanese Ergonomics Society Encouragement Award for Academic Paper in 2007, the 2008 Electrical Engineering/Electronics, Computer, Telecommunication, and Information Technology International Conference (ECTI-CON2008) Best Paper Award and the Fourth International Conference on Innovative Computing, Information and Control Best Paper Award in 2009.